PECULIARITIES OF 3-D FLOW DEVELOPMENT AT IMPINGED AND SWEPT SHOCK WAVE / SURFACE INTERACTIONS

E.K. Derunov, A.A. Zheltovodov, and A.I. Maksimov

Institute of Theoretical and Applied Mechanics SB RAS,
630090 Novosibirsk, Russia

Shock-wave/boundary-layer interactions (SWBLI) arise both in an external supersonic flow around various control surfaces of flying vehicles and in inlet ducts. Numerous situations with 3-D separated turbulent flows are especially complex and actively studied now. Accurate definition of their specific features and search of general properties are important for deeper understanding of their physics and development of computational models. Complex 3-D SWBLI are observed for example in the supersonic flow around the double-fin configuration (DF) mounted on a plate that models an inlet with three-dimensional compression (Fig. 1, *a*) and around the double-body of revolution (DB) over the surface (Fig. 1, *b*). Interaction of swept crossing shock waves (SCSW) and expansion fans is realized in the first case. The second case is characterized by interaction of similar impinged disturbances with the surface. The objective of present study is a comparison of the features in development of such flows under a change of shock waves strength or a distance between the bodies. One of the effective techniques to specify the features of 3-D separation appearance and evolution is an analysis of the surface flow pattern visualization in the interaction regions (obtained by coating the test model surface with an oil film) because their topological properties can be theoretically grounded [1]. For example a theorem is known that defines the number and type of singular points associated with separation and reattachment points as well as vortexes centers. Position of the coalescence and divergence lines which are associated with the boundaries of 3-D separation zones is defined by initial structure of these singular points.

The studies conducted before [2–4] have allowed to reveal specific features of the flows evolution in the vicinity of symmetric ($\beta_1 = \beta_2$) and asymmetric ($\beta_1 \neq \beta_2$) DF configurations (Fig. 1, *a*) at the range of deflection angles $\beta = 7 – 23°$ at different flow nominal Mach numbers $M_\infty = 3$; 4 and 5 under conditions of turbulent boundary layer at the Reynolds number $Re_\delta = (1.4 – 3.2)\cdot 10^5$, where δ – the boundary layer thickness upstream of the fins leading edges. The fins height $h >> \delta$ and the channel width $b/\delta \approx 10$ (at $M_\infty = 3$; 4) and 26 (at $M_\infty = 5$). The results of these studies are the basis for a comparison with the cases of DB interactions. Detailed description of DB test model (Fig. 1, *b*) with two identical cylindrical bodies of

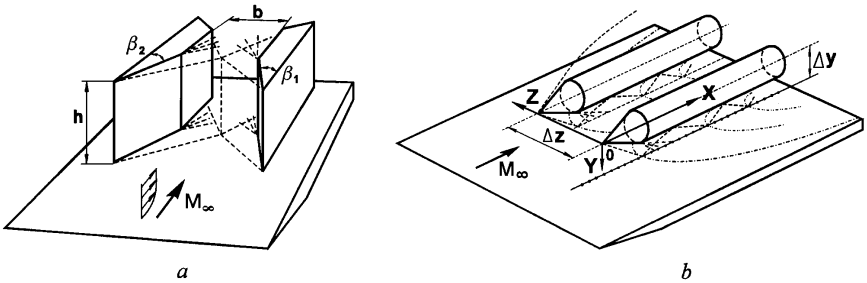

a *b*

Fig. 1. Double-fin (*a*) and double-body (*b*) configurations.

Report Documentation Page

Report Date	Report Type	Dates Covered (from... to)
23 Aug 2002	N/A	-

Title and Subtitle Peculiarities of 3-D Flow Development at Impinged and Swept Shock Wave/Surface Interactions	**Contract Number**
	Grant Number
	Program Element Number
Author(s)	**Project Number**
	Task Number
	Work Unit Number
Performing Organization Name(s) and Address(es) Institute of Theoretical and Applied Mechanics Institutskaya 4/1 Novosibirsk 530090 Russia	**Performing Organization Report Number**
Sponsoring/Monitoring Agency Name(s) and Address(es) EOARD PSC 802 Box 14 FPO 09499-0014	**Sponsor/Monitor's Acronym(s)**
	Sponsor/Monitor's Report Number(s)

Distribution/Availability Statement
Approved for public release, distribution unlimited

Supplementary Notes
See also ADM001433, Conference held International Conference on Methods of Aerophysical Research (11th) Held in Novosibirsk, Russia on 1-7 Jul 2002

Abstract

Subject Terms

Report Classification unclassified	**Classification of this page** unclassified
Classification of Abstract unclassified	**Limitation of Abstract** UU

Number of Pages
7

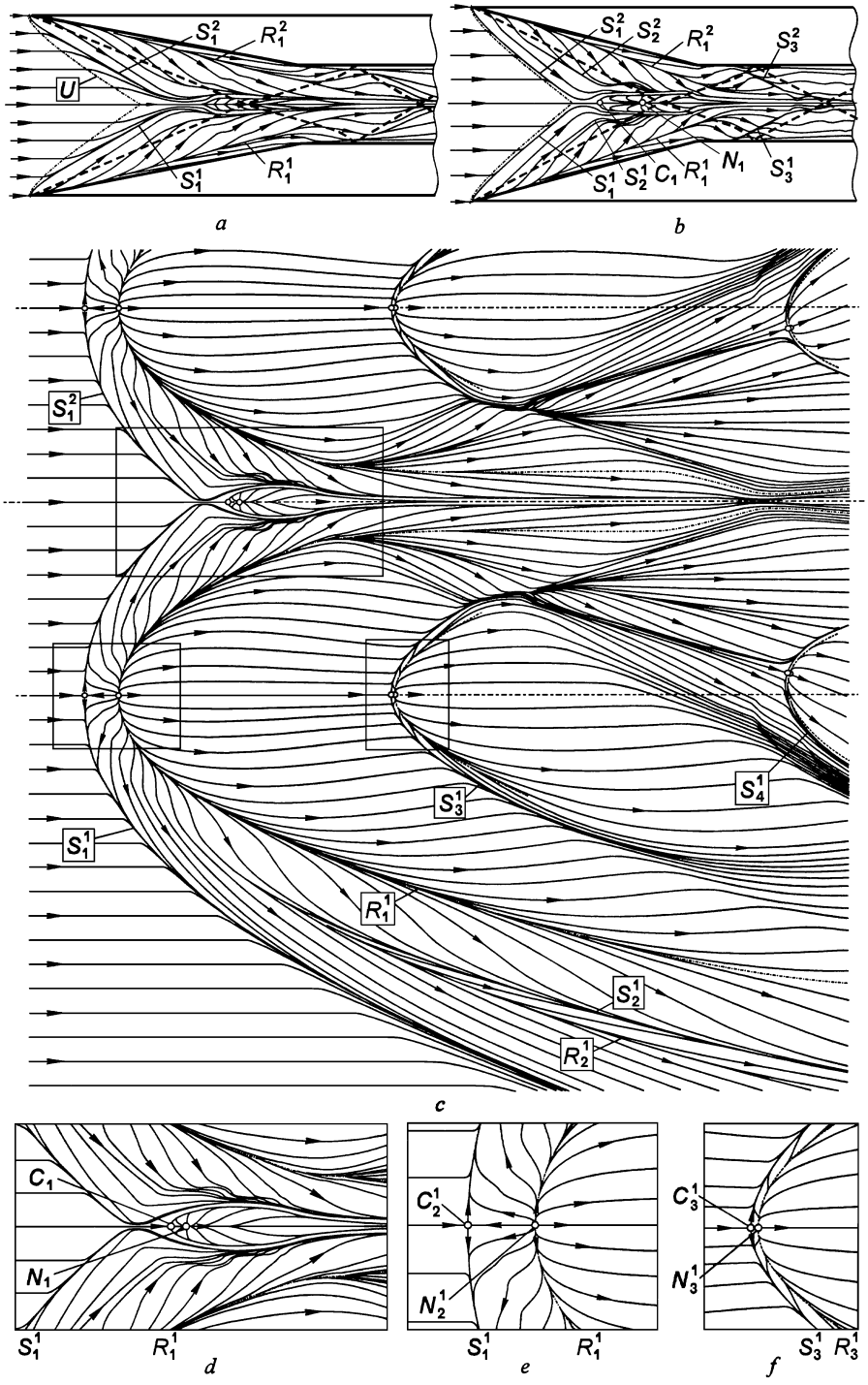

Fig. 2. Surface flow patterns at $M_\infty = 4$ for the DF (*a*: $\beta_1 = \beta_2 = 11°$; *b*: $\beta_1 = \beta_2 = 15°$) and DB (*c* – *f*: $Z = 3.0$) configurations.

revolution (combination of a cone with a semi-apex angle $\beta = 30°$ and a cylinder of diameter $D = 50$ mm) that was used in the experimental studies at $M_\infty = 4$ and $Re_\delta = 1{,}2 \cdot 10^5$ (where $\delta \approx 2.2$ mm – the boundary layer thickness on a plate upstream of impinged bow shock waves) can be found in [5]. The aspect ratio of the cylinder was $\lambda = L/D = 5$, the distance between the axis of every body and plate surface $Y = \Delta y/D = 0.96$, the range of investigated horizontal distances between the bodies $Z = \Delta z/D = 1.06 – 3$.

As the deflection angles β increase unseparated regime of flow between the fins is changed by the stage of the central separation zone appearance in the vicinity of first intersection of the "inviscid" shock waves shown by dotted lines in the figures of limiting streamlines (Fig. 2, *a, b*). This zone is located downstream of the throat that is formed by the primary coalescence (separation) lines S_1^1 and S_1^2 (Fig. 2, *b*). The saddle point C_1 corresponds to the boundary layer separation on the centerline. The node N_1 with the longitudinal divergence line extended from it along the centerline is located downstream. Increase of the angle β leads to the growth of the scale of the central separation zone and to formation of the secondary separation lines S_2^1 and S_2^2 in the flows that spread from the convergence lines R_1^1 and R_1^2. Additional convergence lines S_3^1 and S_3^2 are caused by the shock waves reflected from the side walls of the channel. Similar central separation zone forms also on a plate surface in the case of impinged bow shock waves interaction generated by two bodies of revolution (Fig. 2, *c*). The flow topology in this region is shown in details in Fig. 2, *d*. The bow shock waves stimulate the boundary layer separation under the first and second bodies along the primary coalescence lines S_1^1 and S_1^2 with attachment on the primary divergence line R_1^1 and its symmetric counterpart R_1^2 as well as forming of the secondary coalescence and divergence lines S_2^1, R_2^1 and their symmetric counterparts. Repeated reflection of shock waves between the plate and bodies is the reason of additional coalescence (S_3^1, S_4^1) and divergence (R_3^1, R_4^1) lines and their symmetric counterparts. As is seen, considered coalescence and divergence lines spread respectively from the saddle points C_2^1, C_3^1 and the nodes N_2^1, N_3^1 (Figs. 2, *e, f*).

The centerline surface pressure coincidence in a region between the point of its growth beginning (upstream influence lines *U* intersection point) up to the end of the "plateau" region ($x = 0 – 25$ mm) for DF and DB cases under consideration at the fixed Mach number value additionally confirms similarity of these flows in the regime of developed central separation zone (Fig. 3). Discrepancies in the pressure levels downstream ($x > 25$ mm) are cased by influence of intensive expansion fans that spread from the cone/cylinder junctions of the revolution bodies. Similar influence of expansion fans cased by inflections of the side surfaces of the fins is displayed only at $x > 70$ mm.

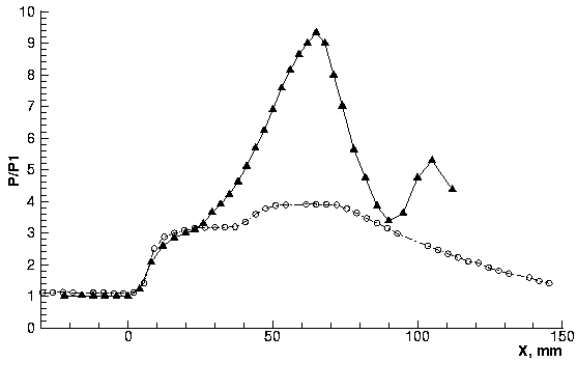

Fig. 3. Flat plate pressure distributions along a centerlines of the DF and DB configurations at $M_\infty = 4$
▲ – DF, $\beta_1 = \beta_2 = 15°$; ○ – DB, $Z = 3.0$

As shown in [4], the primary separation lines S_1^1 and S_1^2 merge and the cross separation line S_3 with the centerline saddle point C_1 appear in result of complex evolution of the flow under the growth of interacted shock waves strength in the DF case (Figs. 4, *a, b*). The reversed flow penetrates from the node N_1 up to the separation

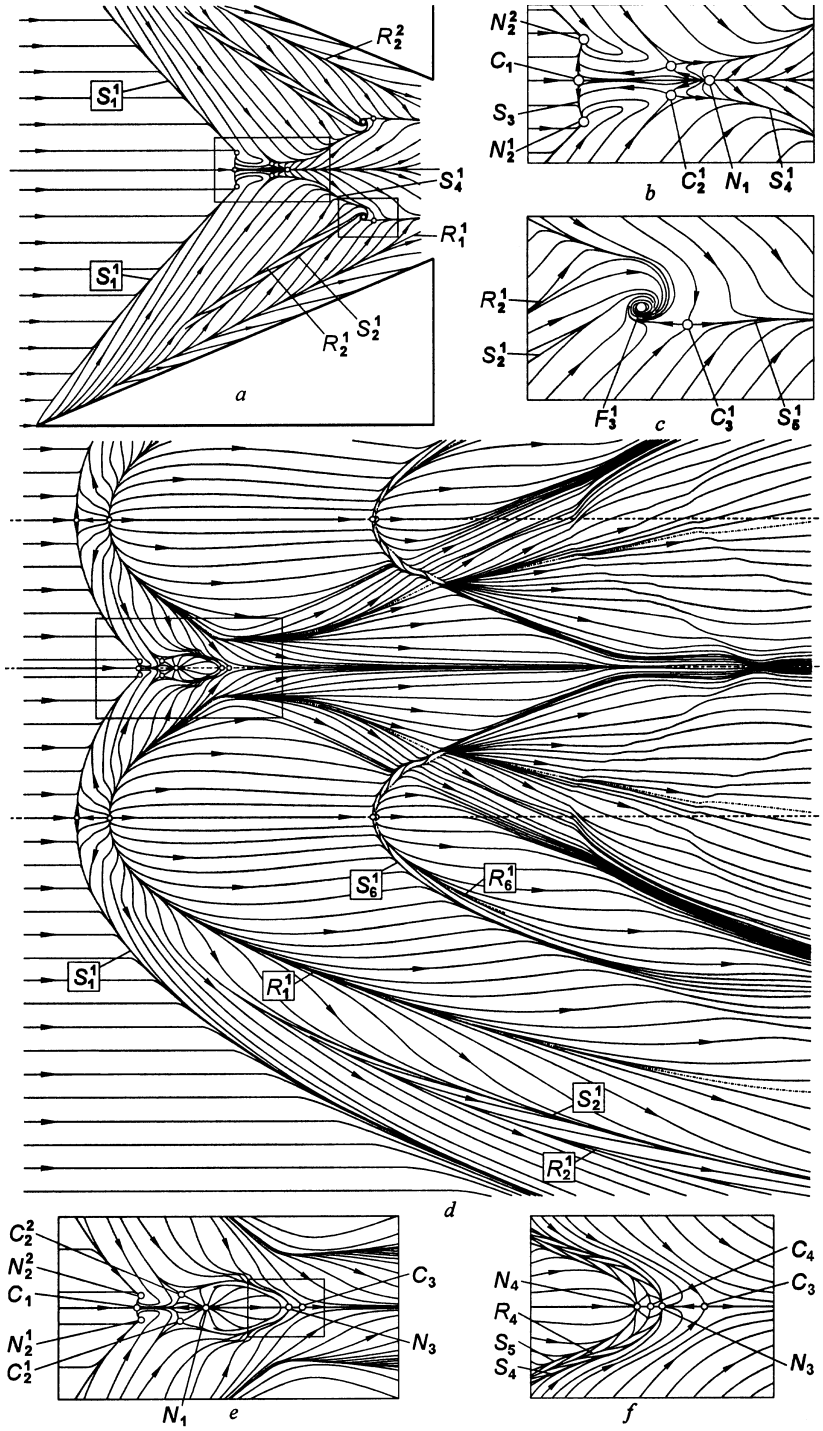

Fig. 4. Surface flow patterns for the DF (*a* – c: $M_\infty = 5$, $\beta_1 = \beta_2 = 23°$) and DB (*d* – *f*: $M_\infty = 4$, $Z = 2.4$) configurations.

line S_3 with appearance of two symmetric nodes N_2^1 and N_2^2 in its ends. Interaction of the secondary flows directed to the central separated zone cases a forming of two additional symmetric saddle points C_2^1 and C_2^2. The foci F_3^1 and the saddle C_3^1 as well as their symmetric counterparts formed in the region of intersection of the secondary separation S_2^1 and attachment R_2^1 lines with the central separation zone.

The flow features described above are discovered also in DB case with decreasing the distance between the bodies up to $Z = 2.4$ (Figs. 4, *d, e*). Surface limiting streamlines patterns (Figs. 4, *e, f*) illustrate the change of the flow topology in the end of the central separated zone comparing with one considered above. The saddle points C_3, C_4 and their corresponding nodes N_3, N_4 with the emergence in these points of separation and attachment lines limited this zone are specific. It should be note that in DF case at $M_\infty = 5$, $\beta_1 = \beta_2 = 18°$ [4] the flow downstream of the separation zone is similar to ones shown in Figs. 2, *a*, *b*.

Further decreasing the distance between the bodies up to $Z = 1.8$ causes increasing the distance between the nodes N_2^1 and N_2^2 as well as displacement of the saddle C_1 and the separation line S_3 upstream (Figs. 5, *a, b*). As seen, the forward separated zone is limited

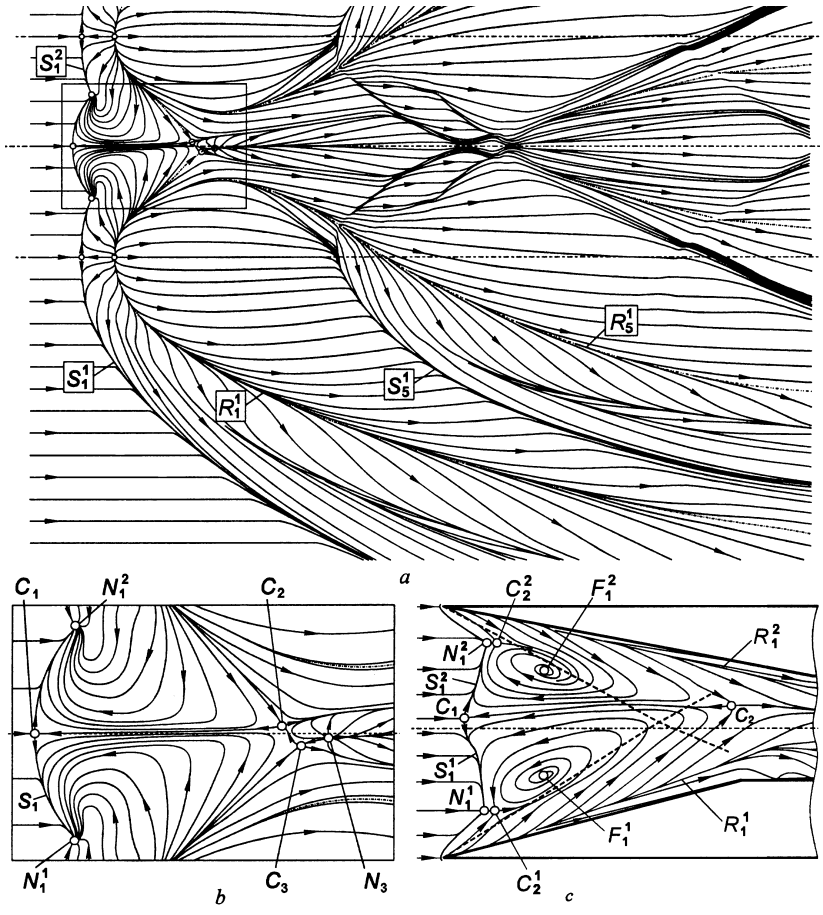

Fig. 5. Surface flow patterns for the DB at $M_\infty = 4$ (*a*, *b*: $Z = 1.8$) and DF at $M_\infty = 3$ (*c*: $\beta_1 = 15°$, $\beta_2 = 11°$).

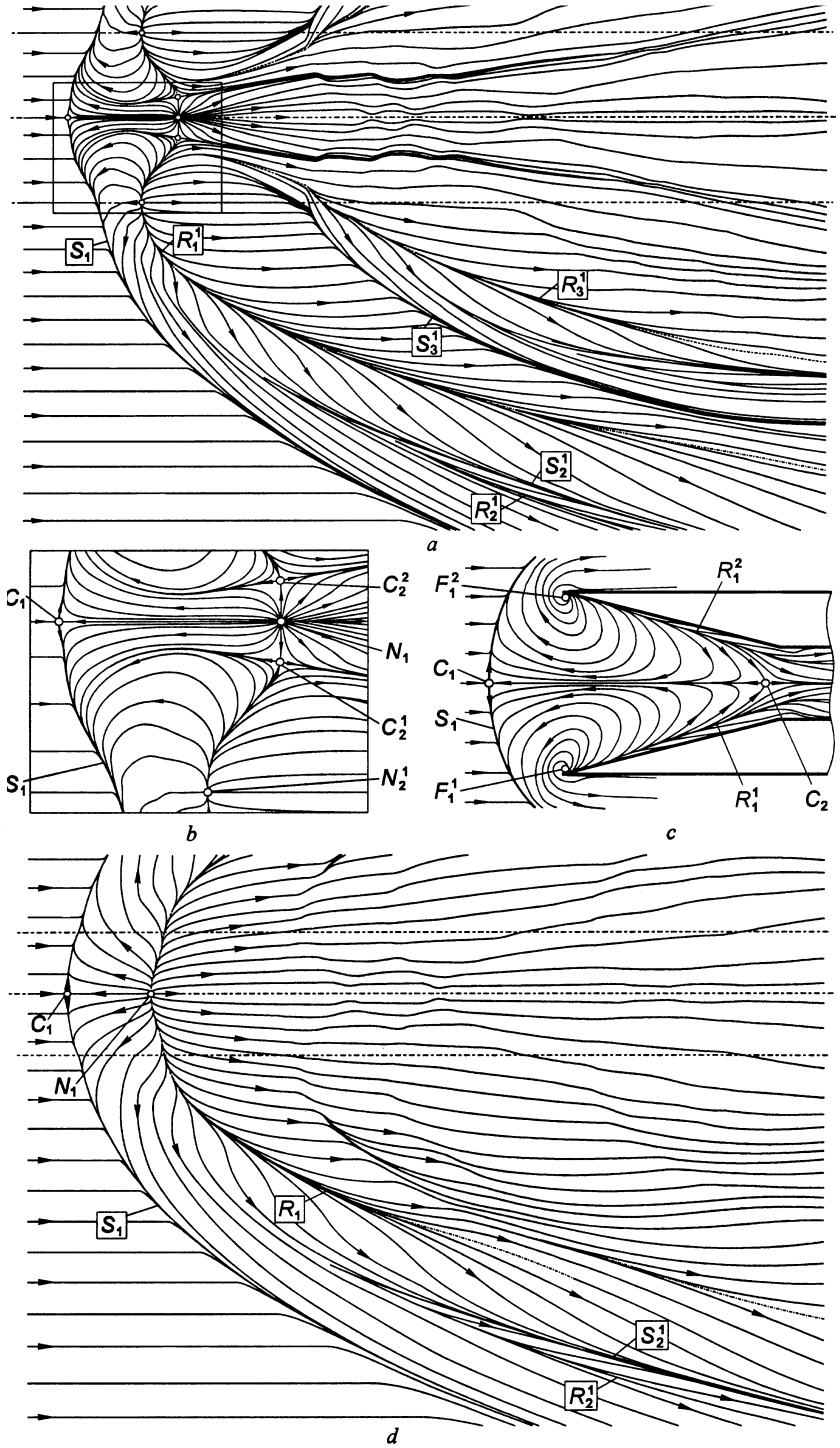

Fig. 6. Surface flow patterns for the DB at $M_\infty = 4$ (*a*, *b*: $Z = 1.4$; *d*: $Z = 1.06$) and DF at $M_\infty = 3$ (*c*: $\beta_1 = \beta_2 = 15°$).

downstream by the saddle C_2. The isolated and asymmetrically located second zone with the saddle C_3 in the apex and the node N_3 downstream is located after it. The reversed flow does not penetrate from the second zone up to the line S_3 at such conditions as it was in previous case. The flow in the first zone reminds one typical for DF at conditions close to the channel choking (Fig. 5, *c*), additional specific features of which are two foci F_1^1, F_1^2 and their correspondent saddle points C_2^1, C_2^2.

Decreasing of the distance between the bodies up to $Z = 1.4$ causes the recovery of the regime when the reversed flow penetrates from the node N_1 up to the separation line S_1 (Fig. 6, *a, b*). Additional saddle points C_2^1, C_2^2 are compensated by the node N_2^1 and it symmetric counterpart N_2^2. Surface flow pattern at $Z = 1.06$ reminds typical one for the case of flow over the single body (Fig. 6, *d*). It should be supposed that such phenomena is caused by the flow choking between the bodies of revolution. Single saddle C_1 is compensated by the node N_1 in this case. The scheme of DF flow for the channel choking regime is shown in Fig. 6, *c*. Topology of such flow is more complex because two saddles C_1, C_2 are compensated by two foci F_1^1, F_1^2.

It should be noted that in all cases under consideration well known topological rule is fulfilled in accordance with which the saddle points are compensated by the nodes and foci [1]. Obtained topological schemes form the basis for verification of numerical computations in a framework of the Reynolds averaged Navier – Stokes equations (RANS) and different turbulence models to predict 3-D flowfield structure and other properties at different conditions. Possibilities of such computations for DF cases have been demonstrated for example in [6–11]. Application of similar approaches for DB cases could specify their flowfield structure. Further specification of the reasons of discovered flow reconstruction at $Z = 1.8$ (Fig. 5, *a, b*) is of interest also, in particular to conclude if it is the result of the flow unsteadiness to the external unsteady disturbances at this regime or it is initiated by some additional factors for example by small asymmetry of flow in result of some deformation of the test model.

REFERENCES

1. **Delery J.M.** Physics of Vortical Flows // J. of Aircraft. 1992. Vol. 29, No. 5. P. 856–876.
2. **Zheltovodov A.A., Maksimov A.I., Shevchenko A.M.** Topology of three-dimensional separation under the conditions of symmetric interaction of crossing shocks and expansion waves with turbulent boundary layer // Thermophys. and Aeromech. 1998. Vol. 5, No. 3. P. 293–312.
3. **Zheltovodov A.A., Maksimov A.I., Shevchenko A.M., Knight D.D.** Topology of three-dimensional separation under the conditions of asymmetrical interaction of crossing shocks and expansion waves with turbulent boundary layer // Thermophys. and Aeromech. 1998. Vol. 5, No. 4. P. 483–503.
4. **Schülein E., Zheltovodov A.A.** Development of experimental methods for the hypersonic flows studies in Ludwieg tube // Intern. Conf. on the Methods of Aerophys. Research: Proc. Pt I. Novosibirsk, Russia 29 June – 3 July, 1998. Novosibirsk, 1998. P. 191–199.
5. **Brodetsky M.D., Derunov E.K., Kharitonov A.M., Zabrodin A.V., Lutsky A.E.** Interference in a supersonic flow around a combination of bodies. 2. The flow around two bodies of revolution over a flat surface // Thermophys. and Aeromech. 1999. Vol. 6, No. 2. P. 151–157.
6. **Knight D., Yan H., Panaras A., Zheltovodov A.** RTO WG 10: CFD validation for shock wave turbulent boundary layer Interactions // AIAA 2002-0437, 30 p.
7. **Thivet F., Knight D.D., Zheltovodov A.A., Maksimov A.I.** Insights in turbulence modeling for crossing-shock-wave/boundary layer interactions // AIAA J. 2001. Vol. 39, No. 6. P. 985–995.
8. **Zheltovodov A.A., Maksimov A.I., Gaitonde D.V., Visbal M.R., Shang J.S.** Experimental and numerical studies of symmetric crossing-shock-wave / turbulent boundary layer interaction // Thermophys. and Aeromech. 2000. Vol. 7, No 2. P. 155–171.
9. **Gaitonde D.V., Visbal M.R., Shang J.S., Zheltovodov A.A., Maksimov A.I.** Sidewall interaction in an asymmetric simulated scramjet inlet configuration // J. of Propulsion and Power. 2001. Vol. 17, No. 3. P. 579–584.
10. **Zheltovodov A.A., Maksimov A.I., Schülein E., Gaitonde D.V., Schmisseur J.D.** Verification of crossing-shock-wave/boundary layer interaction computations with the k - ε turbulence model // Intern. Conf. on the Methods of Aerophys. Research: Proc. Pt I. Novosibirsk, Russia 9 June – 3 July, 2000. Novosibirsk, 2000. P. 231–241.
11. **Knight D., Gnedin M., Becht R., Zheltovodov A.** Numerical simulation of crossing-shock-wave/turbulent-boundary-layer interaction using a two-equation model of turbulence // J. Fluid Mech. 2000. Vol. 409. P. 121–147.